IRS-Assisted Interference Mitigation for Full-Duplex IAB Network

Seok-Hyun Yoon, Byungju Lim, and Young-Chai Ko, *Senior Member, IEEE*

***Abstract*—This letter studies intelligent reflecting surface (IRS)-aided full-duplex (FD) integrated access and backhaul (IAB) network, where IRSs are deployed near small-cell base stations (SBSs) to mitigate several types of interference including self-interference in FD system. An optimization problem is formulated to maximize network throughput by jointly optimizing precoder at base stations (BSs) for establishing wireless backhaul and access links, and passive beamforming at IRSs. To solve this non-convex problem, we divide the problem into two subproblems by using the relationship between data rate and weighted rate-minimum mean square error (WMMSE). Then, we propose the block coordinate descent (BCD) algorithm, where the BS precoder is optimized using quadratically constrained quadratic programming (QCQP) and the IRS passive beamforming is obtained via semi-definite relaxation (SDR) method. Simulation results illustrate that our proposed algorithm can effectively mitigate interference with the help of IRSs and achieve a better sum rate performance compared to conventional schemes.**

***Index Terms*—IAB network, full-duplex, IRS, 6G.**

I. Introduction

TO REDUCE the cost of installing small-cell base stations (SBSs) and enhance spectral efficiency, full-duplex (FD) integrated access and backhaul (IAB) network has emerged as an appealing solution, where SBSs can simultaneously transmit and receive through both backhaul and access links [1]. However, the benefits of FD IAB network are limited due to two additional interference sources: 1) self-interference and 2) cross-tier interference. First, the received backhaul link signal suffers from self-interference (SI), which is caused by the direct reception of access link signal at each SBS. Second, interference from MBS to user equipments (UEs) and inter-SBS interference are introduced in FD system, which is referred as cross-tier interference. To mitigate these interferences, beamforming or power control methods can be used [2]. However, since SI power is relatively high due to a very close distance and degrades the quality of received signals, efficient SI cancellation (SIC) methods are additionally required [1]. Existing SIC methods consist of three main steps: 1) propagation domain cancellation, 2) analog domain cancellation, and 3) digital domain cancellation. These steps effectively cancel out SI, but it incurs a high cost and power consumption due to additional active components and circuits. In particular, analog SIC, which suppresses SI power below the dynamic range of analog-to-digital converter (ADC), is constrained by its frequency-selective nature and the large insertion loss of analog SIC circuits [3]. Thus, an alternative technique to mitigate SI is needed instead of analog SIC.

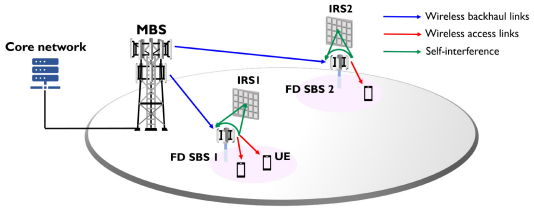


Fig. 1. Two-tier IRS-Assisted full-duplex IAB system.

Intelligent reflecting surface (IRS), which is composed of a large number of passive elements, has emerged as a key technology to dynamically reconfigure wireless channel, resulting in interference mitigation in IRS assisted network [4], [5]. Recent works have tried to exploit the characteristics of IRS for SI mitigation in FD system instead of conventional SIC methods [6], [7]. By jointly optimizing base station (BS) active beamforming and IRS passive beamforming, SI power can be minimized while enhancing channel gain to improve spectral efficiency. However, the above works focused on single-cell FD or multi-cell HD system, which may not be directly applicable in multi-cell FD IAB networks, where various types of interference exist such as SI and cross-tier interference.

In this letter, we study an interference mitigation method in IRS-assisted multi-cell FD IAB network for replacing the analog domain SIC while suppressing other interferences. In contrast to previous studies, we optimize IRS passive beamforming by considering all the interferences in an IAB network. We first formulate an optimization problem to maximize network throughput, and then we adopt a weighted rate-minimum mean square error (WMMSE) approach to optimize both the BS precoder and the IRS passive beamforming. Specifically, the BS precoder is optimized via quadratically constrained quadratic programming (QCQP) while the IRS passive beamforming is obtained using semi-definite relaxation (SDR) method with Gaussian randomization. Simulation results demonstrate that the proposed scheme outperforms the conventional schemes and we verify the effectiveness of IRS to mitigate interference in an FD IAB network.

II. System Model and Problem Formulation

We consider the two-tier downlink IAB system where an MBS connected to a core network provides wireless backhaul links to L SBSs, as in Fig. 1. In this network, each SBS operates in FD mode, enabling it to receive the backhaul link signal from MBS and transmit the access link signals to K

Manuscript received 19 January 2024; revised 7 March 2024; accepted 4 April 2024. Date of publication 8 April 2024; date of current version 11 June 2024. This work was supported in part by the Pukyong National University Research Fund in 2023 under Grant 202303820001, and in part by the Institute of Information and Communications Technology Planning and Evaluation (IITP) Grant funded by the Korea Government (MSIT) under Grant 2021-0-00260 (Research on LEO Inter-Satellite Links). The associate editor coordinating the review of this article and approving it for publication was F. Shu. *(Corresponding author: Byungju Lim.)*

Seok-Hyun Yoon and Young-Chai Ko are with the School of Electrical Engineering, Korea University, Seoul 02841, South Korea (e-mail: daniel419@korea.ac.kr; koyc@korea.ac.kr).

Byungju Lim is with the Department of Electronic Engineering, Pukyong National University, Busan 48513, South Korea (e-mail: limbj@pknu.ac.kr).

Digital Object Identifier 10.1109/LWC.2024.3386209

2162-2345 © 2024 IEEE. Personal use is permitted, but republication/redistribution requires IEEE permission.
See https://www.ieee.org/publications/rights/index.html for more information.

Authorized licensed use limited to: Univ Of Incheon. Downloaded on October 26,2026 at 13:13:39 UTC from IEEE Xplore. Restrictions apply.

single-antenna UEs over the same time-frequency resources. MBS is equipped with N_{M} antennas, and each SBS has N_{S} antennas for access link while single antenna is used for backhaul link. To mitigate SI and enhance the performance of the desired links, one IRS with N_{I} passive elements is deployed in the vicinity of each SBS. We denote the index of MBS as 0, and the set of SBSs are represented as $\mathcal{L} \triangleq \{1, 2, \ldots, L\}$. The k-th UE associated with the l-th SBS is denoted as l_k. In addition, $\Theta_l = \mathsf{diag}(\theta_{l,1}, \ldots, \theta_{l,N})$ is defined as the passive beamforming matrix for IRS in the vicinity of the l-th SBS with $|\theta_{l,n}| = 1$.

We denote the channels from MBS to the l-th SBS, the l-th IRS, and the l_k-th UE as $\mathbf{h}_{0,l}^d \in \mathbb{C}^{1\times N_{\mathsf{M}}}$, $\mathbf{G}_{0,l} \in \mathbb{C}^{N_{\mathsf{I}}\times N_{\mathsf{M}}}$ and $\mathbf{f}_{0,l_k}^d \in \mathbb{C}^{1\times N_{\mathsf{M}}}$; the channels from the j-th SBS to the l-th SBS, the l-th IRS, and the l_k-th UE as $\mathbf{h}_{j,l}^d \in \mathbb{C}^{1\times N_{\mathsf{S}}}$, $\mathbf{G}_{j,l} \in \mathbb{C}^{N_{\mathsf{I}}\times N_{\mathsf{S}}}$ and $\mathbf{f}_{j,l_k}^d \in \mathbb{C}^{1\times N_{\mathsf{S}}}$; the channels from the j-th IRS to the l-th SBS and the l_k-th UE as $\mathbf{h}_{j,l}^r \in \mathbb{C}^{1\times N_{\mathsf{I}}}$ and $\mathbf{f}_{j,l_k}^r \in \mathbb{C}^{1\times N_{\mathsf{I}}}$, respectively. Due to severe multiplicative path-loss in the multi-IRS network, we only consider a single-hop reflected path. Also, we denote $\theta_l = [\theta_{l,1}, \ldots, \theta_{l,N}]^{\mathsf{H}}$, $\mathbf{A}_{0,l,l} = \mathsf{diag}(\mathbf{h}_{l,l}^r)\mathbf{G}_{0,l}$, $\mathbf{A}_{j,i,l} = \mathsf{diag}(\mathbf{h}_{i,l}^r)\mathbf{G}_{j,i}$, and $\mathbf{A}_{j,l_k}^{\mathsf{UE}} = \mathsf{diag}(\mathbf{f}_{j,l_k}^r)\mathbf{G}_{j,j}$. We assume that perfect channel information can be obtained at each BS by using existing methods for estimating the effective channel including cascaded channel through IRSs [8] and SI channel [9].

Let us denote $\mathbf{s}^{\mathsf{B}} \triangleq [s_1^{\mathsf{B}}, \ldots, s_L^{\mathsf{B}}]^{\mathsf{T}}$ and $\mathbf{s}_l^{\mathsf{A}} \triangleq [s_{l_1}^{\mathsf{A}}, \ldots, s_{l_K}^{\mathsf{A}}]^{\mathsf{T}}$ as the transmit symbol vector at MBS and the l-th SBS, with zero mean and unit variance. Additionally, the transmit precoder at MBS and the l-th SBS are denoted as $\mathbf{V} \triangleq [\mathbf{v}_1, \ldots, \mathbf{v}_L]$ and $\mathbf{W}_l \triangleq [\mathbf{w}_{l_1}, \ldots, \mathbf{w}_{l_K}]$, respectively. Then, the received backhaul signal at the l-th SBS is given by

$$y_l^{\mathsf{B}} = \underbrace{\bar{\mathbf{h}}_{0,l}\mathbf{v}_l s_l^{\mathsf{B}}}_{\text{desired signal}} + \underbrace{\sum_{j\neq l}^{L} \bar{\mathbf{h}}_{0,l}\mathbf{v}_j s_j^{\mathsf{B}}}_{\text{inter-bakchaul interference}} + \underbrace{\sum_{j\neq l}^{L} \bar{\mathbf{h}}_{j,l}\mathbf{W}_j \mathbf{s}_j^{\mathsf{A}}}_{\text{inter-SBS interference}} + \underbrace{\bar{\mathbf{h}}_{\mathsf{SI},l}\mathbf{W}_l\mathbf{s}_l^{\mathsf{A}}}_{\text{self-interference}} + \underbrace{n_l^{\mathsf{B}}}_{\text{noise}}, \tag{1}$$

where $\bar{\mathbf{h}}_{0,l} = \mathbf{h}_{0,l}^d + \theta_l^{\mathsf{H}}\mathbf{A}_{0,l,l}$ is the effective channel from MBS to the l-th SBS, $\bar{\mathbf{h}}_{j,l} = \mathbf{h}_{j,l}^d + \theta_j^{\mathsf{H}}\mathbf{A}_{j,j,l} + \theta_l^{\mathsf{H}}\mathbf{A}_{j,l,l}$, $j \neq l$, is the effective channel from the j-th SBS to the l-th SBS, $\bar{\mathbf{h}}_{\mathsf{SI},l} = \mathbf{h}_{l,l}^d + \theta_l^{\mathsf{H}}\mathbf{A}_{l,l,l}$ is the effective SI channel, and $n_l^{\mathsf{B}} \sim \mathcal{CN}(0, \sigma^2)$ is the additive white Gaussian noise (AWGN). Note that ADC saturation may be introduced by excessive SI power. Hence, it is imperative to jointly design the SBS precoder $\mathbf{W}_l$ and the IRS passive beamforming θ_l to suppress the SI power below the dynamic range of ADC, and the SI power regulation is expressed as

$$\|\bar{\mathbf{h}}_{\mathsf{SI},l}\mathbf{W}_l\|^2 \leq \eta_{\mathsf{ADC}},\ \forall l \in \mathcal{L}, \tag{2}$$

where $\eta_{\mathsf{ADC}} = \sigma^2 + 6.021 \cdot b + 1.763 - 10\,(\mathrm{dB})$ represents the power threshold of b-bit ADC determined by its dynamic range [10]. Then, the quantized backhaul signal at the l-th SBS after passing through ADC is given by

$$y_{\mathsf{q},l}^{\mathsf{B}} = \alpha_l y_l^{\mathsf{B}} + n_{\mathsf{q},l}^{\mathsf{B}}, \tag{3}$$

where $\alpha_l = 1 - \beta_l$ is the quantization loss with $\beta_l = \frac{\pi\sqrt{3}}{2}2^{-2b}$ and $n_{\mathsf{q},l}^{\mathsf{B}}$ is the quantization noise with variance $\sigma_{\mathsf{q},l}^2$, which is defined as

$$\begin{aligned}\sigma_{\mathsf{q},l}^2 &= \alpha_l\beta_l\mathbb{E}\{|y_l^{\mathsf{B}}|^2\} \\ &= \alpha_l\beta_l\big(\|\bar{\mathbf{h}}_{0,l}\mathbf{V}\|^2 + \sum_{j\neq l}^{L}\|\bar{\mathbf{h}}_{j,l}\mathbf{W}_j\|^2 + \|\bar{\mathbf{h}}_{\mathsf{SI},l}\mathbf{W}_l\|^2 + \sigma^2\big).\end{aligned} \tag{4}$$

It is noted that the SI component $\alpha_l\bar{\mathbf{h}}_{\mathsf{SI},l}\mathbf{W}_l\mathbf{s}_l^{\mathsf{A}}$ in (3) can be estimated and canceled out via a digital SIC method. Then, the residual backhaul signal of the l-th SBS can be written by

$$y_{\mathsf{r},l}^{\mathsf{B}} = \alpha_l\left(\bar{\mathbf{h}}_{0,l}\mathbf{v}_l s_l^{\mathsf{B}} + \sum_{j\neq l}^{L}\bar{\mathbf{h}}_{0,l}\mathbf{v}_j s_j^{\mathsf{B}} + \sum_{j\neq l}^{L}\bar{\mathbf{h}}_{j,l}\mathbf{W}_j\mathbf{s}_j^{\mathsf{A}} + n_l^{\mathsf{B}}\right) + n_{\mathsf{q},l}^{\mathsf{B}} + n_{\mathsf{r},l}^{\mathsf{B}}. \tag{5}$$

where $n_{\mathsf{r},l}^{\mathsf{B}} \sim \mathcal{CN}(0, \sigma_{\mathsf{r},l}^2)$ is the residual self-interference.

The received access signal at the l_k-th UE is given by

$$y_{l_k}^{\mathsf{A}} = \underbrace{\bar{\mathbf{f}}_{l,l_k}\mathbf{w}_{l_k}s_{l_k}^{\mathsf{A}}}_{\text{desired signal}} + \underbrace{\sum_{m\neq k}^{K}\bar{\mathbf{f}}_{l,l_k}\mathbf{w}_{l_m}s_{l_m}^{\mathsf{A}}}_{\text{intra-cell interference}} + \underbrace{\sum_{j\neq l}^{L}\bar{\mathbf{f}}_{j,l_k}\mathbf{W}_j\mathbf{s}_j^{\mathsf{A}}}_{\text{inter-cell interference}} + \underbrace{\mathbf{f}_{0,l_k}^d\mathbf{V}\mathbf{s}^{\mathsf{B}}}_{\text{interference from MBS}} + \underbrace{n_{l_k}^{\mathsf{A}}}_{\text{noise}}. \tag{6}$$

where $\bar{\mathbf{f}}_{j,l_k} = \mathbf{f}_{j,l_k}^d + \theta_j^{\mathsf{H}}\mathbf{A}_{j,l_k}^{\mathsf{UE}}, j \neq 0$ is the effective channel from the j-th SBS to the l_k-th UE. Based on (5) and (6), the achievable rate of the l-th SBS for backhaul link and the l_k-th UE for access link can be written as (7) and (8), shown at the bottom of the next page. To maximize the system sum rate, we jointly optimize the precoder at the MBS $\mathbf{V}$ and at the SBSs $\mathbf{W}_l$, and the IRS passive beamforming θ_l, and its optimization problem can be formulated as

$$\max_{\mathbf{V},\mathbf{W}_l,\theta_l}\ \sum_{l=1}^{L}\min\left\{R_l^{\mathsf{B}}, \sum_{k=1}^{K}R_{l_k}^{\mathsf{A}}\right\} \tag{9a}$$

$$\text{s.t.}\ \ \|\mathbf{V}\|_{\mathrm{F}}^2 \leq P_{\mathsf{M}}, \tag{9b}$$

$$\|\mathbf{W}_l\|_{\mathrm{F}}^2 \leq P_{\mathsf{S}},\ \forall l \in \mathcal{L}, \tag{9c}$$

$$\|\bar{\mathbf{h}}_{\mathsf{SI},l}\mathbf{W}_l\|^2 \leq \eta_{\mathsf{ADC}},\ \forall l \in \mathcal{L}, \tag{9d}$$

$$|\theta_{l,n}| = 1,\ n = 1, 2, \ldots, N. \tag{9e}$$

The constraints (9b) and (9c) represent the transmit power constraint at MBS and SBS with the maximum transmit power P_{M} and P_{S}, respectively. The problem (9) is a non-convex since the optimization variables are highly coupled in the objective function with the non-convex unit amplitude constraint (9e). Additionally, since the objective function is non-differentiable, the conventional algorithm in [11] cannot be applied. Thus, to address this difficulty, we reformulate it into a smooth and tractable form using WMMSE approach and propose block coordinate descent (BCD) method in the following section.

III. Proposed Method

A. Problem Reformulation With WMMSE Approach

To deal with the non-convex objective function with respect to $\mathbf{V}, \mathbf{W}_l$, and θ_l, we adopt the WMMSE approach that transforms the non-convex problem in a tractable form by

Authorized licensed use limited to: Univ Of Incheon. Downloaded on October 26,2026 at 13:13:39 UTC from IEEE Xplore. Restrictions apply.

leveraging the relationship between MMSE and data rate [12]. We first define the scalar equalizers on the received signal at the l-th SBS, $y^{\mathsf{B}}_{\mathsf{q},l}$, and on the received signal at the l_k-th UE, $y^{\mathsf{A}}_{l_k}$, as g^{B}_l and $g^{\mathsf{A}}_{l_k}$, respectively. Then, the mean-squared errors (MSE) of the detected symbol over backhaul link and access link can be expressed as

$$\varepsilon^{\mathsf{B}}_l = \mathbb{E}\{|g^{\mathsf{B}}_l y^{\mathsf{B}}_{l,\mathsf{r}} - s^{\mathsf{B}}_l|^2\} = |g^{\mathsf{B}}_l|^2 T^{\mathsf{B}}_l - 2\,\mathrm{Re}\{g^{\mathsf{B}}_l \alpha_l \bar{\mathbf{h}}_{0,l}\mathbf{v}_l\} + 1, \quad (10)$$

$$\varepsilon^{\mathsf{A}}_{l_k} = \mathbb{E}\{|g^{\mathsf{A}}_{l_k} y^{\mathsf{A}}_{l_k} - s^{\mathsf{A}}_{l_k}|^2\} = |g^{\mathsf{A}}_{l_k}|^2 T^{\mathsf{A}}_{l_k} - 2\,\mathrm{Re}\{g^{\mathsf{A}}_{l_k} \bar{\mathbf{f}}_{l,l_k}\mathbf{w}_{l_k}\} + 1. \quad (11)$$

where

$$T^{\mathsf{B}}_l = \alpha_l\left(\|\bar{\mathbf{h}}_{0,l}\mathbf{V}\|^2 + \textstyle\sum_{j\neq l}^{L}\|\bar{\mathbf{h}}_{j,l}\mathbf{W}_j\|^2 + \beta_l\|\bar{\mathbf{h}}_{\mathsf{SI},l}\mathbf{W}_l\|^2 + \sigma^2\right) + \sigma^2_{l,\mathsf{r}}, \quad (12)$$

$$T^{\mathsf{A}}_{l_k} = \textstyle\sum_{j=l}^{L}\|\bar{\mathbf{f}}_{j,l_k}\mathbf{W}_j\|^2 + \|\bar{\mathbf{f}}_{0,l_k}\mathbf{V}\|^2 + \sigma^2. \quad (13)$$

The optimal equalizers minimizing (10) and (11) can be derived by solving the first-order condition, i.e., $\partial\varepsilon^{\mathsf{B}}_l/\partial g^{\mathsf{B}}_l = 0$ and $\partial\varepsilon^{\mathsf{A}}_{l_k}/\partial g^{\mathsf{A}}_{l_k} = 0$, and the solutions can be obtained as

$$g^{\mathsf{B}}_{l,\mathsf{mmse}} = \alpha_l \mathbf{v}^{\mathsf{H}}_l \bar{\mathbf{h}}^{\mathsf{H}}_{0,l}/T^{\mathsf{B}}_l,\ g^{\mathsf{A}}_{l_k,\mathsf{mmse}} = \mathbf{w}^{\mathsf{H}}_{l_k}\bar{\mathbf{f}}^{\mathsf{H}}_{l,l_k}/T^{\mathsf{A}}_{l_k}. \quad (14)$$

By substituting (14) into (10) and (11), the minimum MSE (MMSE) can be given by

$$\varepsilon^{\mathsf{B}}_{l,\mathsf{mmse}} = 1 - \alpha^2_l|\bar{\mathbf{h}}_{0,l}\mathbf{v}_l|^2/T^{\mathsf{B}}_l,\ \varepsilon^{\mathsf{A}}_{l_k,\mathsf{mmse}} = 1 - |\bar{\mathbf{f}}_{l,l_k}\mathbf{w}_{l_k}|^2/T^{\mathsf{A}}_{l_k}. \quad (15)$$

Let us define auxiliary variables ρ^{B}_l and $\rho^{\mathsf{A}}_{l_k}$ for the l-th SBS and the l_k-th UE, respectively. Then, based on [12], we have

$$R^{\mathsf{B}}_l = \max_{g^{\mathsf{B}}_l,\rho^{\mathsf{B}}_l}\left(\frac{\ln\left(\rho^{\mathsf{B}}_l\right) - \rho^{\mathsf{B}}_l\varepsilon^{\mathsf{B}}_l + 1}{\ln 2}\right),\ R^{\mathsf{A}}_{l_k} = \max_{g^{\mathsf{A}}_{l_k},\rho^{\mathsf{A}}_{l_k}}\left(\frac{\ln\left(\rho^{\mathsf{A}}_{l_k}\right) - \rho^{\mathsf{A}}_{l_k}\varepsilon^{\mathsf{A}}_{l_k} + 1}{\ln 2}\right). \quad (16)$$

Using (16), (9) can be transformed as

$$\max_{\substack{t_l,\mathbf{V},\mathbf{W}_l,\theta_i\\ g^{\mathsf{B}}_l,\rho^{\mathsf{B}}_l,g^{\mathsf{A}}_{l_k},\rho^{\mathsf{A}}_{l_k}}} \quad \sum_{l=1}^{L} t_l \quad (17a)$$

$$\text{s.t.} \quad \ln\left(\rho^{\mathsf{B}}_l\right) - \rho^{\mathsf{B}}_l\varepsilon^{\mathsf{B}}_l + 1 \geq t_l \ln 2,\ \forall l \in \mathcal{L}, \quad (17b)$$

$$\sum_{k=1}^{K}\left(\ln\left(\rho^{\mathsf{A}}_{l_k}\right) - \rho^{\mathsf{A}}_{l_k}\varepsilon^{\mathsf{A}}_{l_k} + 1\right) \geq t_l \ln 2,\ \forall l \in \mathcal{L}, \quad (17c)$$

(9b)-(9e).

Note that the problems in (9) and (17) are equivalent since the KKT conditions of these problems can be satisfied in the same stationary points [12]. To solve (17), we adopt the BCD method which alternately updates optimization variables over each iteration. With fixed $\mathbf{V}, \mathbf{W}_l$ and θ_l, the optimal solutions of $g^{\mathsf{B}}_l, \rho^{\mathsf{B}}_l, g^{\mathsf{A}}_{l_k}$ and $\rho^{\mathsf{A}}_{l_k}$ can be obtained as

$$\left(g^{\mathsf{B}}_l\right)^\star = g^{\mathsf{B}}_{l,\mathsf{mmse}},\ \left(\rho^{\mathsf{B}}_l\right)^\star = 1/\varepsilon^{\mathsf{B}}_{l,\mathsf{mmse}}, \quad (18)$$

$$\left(g^{\mathsf{A}}_{l_k}\right)^\star = g^{\mathsf{A}}_{l_k,\mathsf{mmse}},\ \left(\rho^{\mathsf{A}}_{l_k}\right)^\star = 1/\varepsilon^{\mathsf{A}}_{l_k,\mathsf{mmse}}. \quad (19)$$

It is noted that ρ^{B}_l and $\rho^{\mathsf{A}}_{l_k}$ is a function of MMSE. Then, we propose the algorithms for obtaining $\mathbf{V}, \mathbf{W}_l$ and θ_l in the following section.

B. Precoding Optimization

Let us define $\mathbf{v} \triangleq [\mathbf{v}^{\mathsf{T}}_1, \ldots, \mathbf{v}^{\mathsf{T}}_L]^{\mathsf{T}}$, $\mathbf{w}_l \triangleq [\mathbf{w}^{\mathsf{T}}_{l_1}, \ldots, \mathbf{w}^{\mathsf{T}}_{l_K}]^{\mathsf{T}}$, and $\mathbf{e}_k$ as a vector with $[\mathbf{e}_k]_k = 1$ and $[\mathbf{e}_k]_m = 0$ for $m \neq k$. By substituting (10) and (11) into the problem (17), we can rewrite the constraints (17b), (17c) and (9d) with respect to $\mathbf{v}$ and $\mathbf{w}_l$, respectively, as

$$\mathbf{v}^{\mathsf{H}}\mathbf{X}^{\mathsf{B}}_l\mathbf{v} + \sum_{j\neq l}^{L}\mathbf{w}^{\mathsf{H}}_j\mathbf{X}^{\mathsf{A}}_{j,l}\mathbf{w}_j + \mathbf{w}^{\mathsf{H}}_l\mathbf{X}^{\mathsf{SI}}_l\mathbf{w}_l - 2\mathrm{Re}\{\mathbf{z}^{\mathsf{B}}_l\mathbf{v}\} + t_l\ln 2 \leq c^{\mathsf{B}}_l, \forall l \in \mathcal{L}, \quad (20a)$$

$$\mathbf{v}^{\mathsf{H}}\mathbf{Y}^{\mathsf{B}}_l\mathbf{v} + \sum_{j=1}^{L}\mathbf{w}^{\mathsf{H}}_j\mathbf{Y}^{\mathsf{A}}_{j,l}\mathbf{w}_j - 2\mathrm{Re}\{\mathbf{z}^{\mathsf{A}}_l\mathbf{w}_l\} + t_l\ln 2 \leq c^{\mathsf{A}}_l, \forall l \in \mathcal{L}, \quad (20b)$$

$$\mathbf{w}^{\mathsf{H}}_l\mathbf{Y}^{\mathsf{SI}}_l\mathbf{w}_l \leq \eta_{\mathsf{ADC}}, \forall l \in \mathcal{L}. \quad (20c)$$

where

$$\begin{aligned}
\mathbf{X}^{\mathsf{B}}_l &= \rho^{\mathsf{B}}_l|g^{\mathsf{B}}_l|^2\alpha_l\mathbf{I}_L \otimes \left(\bar{\mathbf{h}}^{\mathsf{H}}_{0,l}\bar{\mathbf{h}}_{0,l}\right), \mathbf{X}^{\mathsf{A}}_{j,l} = \rho^{\mathsf{B}}_l|g^{\mathsf{B}}_l|^2\alpha_l\mathbf{I}_K \otimes \left(\bar{\mathbf{h}}^{\mathsf{H}}_{j,l}\bar{\mathbf{h}}_{j,l}\right),\\
\mathbf{X}^{\mathsf{SI}}_l &= \rho^{\mathsf{B}}_l|g^{\mathsf{B}}_l|^2\alpha_l\beta_l\mathbf{I}_K \otimes \left(\bar{\mathbf{h}}^{\mathsf{H}}_{\mathsf{SI},l}\bar{\mathbf{h}}_{\mathsf{SI},l}\right), \mathbf{Y}^{\mathsf{SI}}_l = \mathbf{I}_K \otimes \left(\bar{\mathbf{h}}^{\mathsf{H}}_{\mathsf{SI},l}\bar{\mathbf{h}}_{\mathsf{SI},l}\right)\\
\mathbf{Y}^{\mathsf{B}}_l &= \textstyle\sum_{k=1}^{K}\left(\rho^{\mathsf{A}}_{l_k}|g^{\mathsf{A}}_{l_k}|^2\mathbf{I}_K \otimes \left(\bar{\mathbf{f}}^{\mathsf{H}}_{0,l_k}\bar{\mathbf{f}}_{0,l_k}\right)\right),\\
\mathbf{Y}^{\mathsf{A}}_{j,l} &= \textstyle\sum_{k=1}^{K}\left(\rho^{\mathsf{A}}_{l_k}|g^{\mathsf{A}}_{l_k}|^2\mathbf{I}_K \otimes \left(\bar{\mathbf{f}}^{\mathsf{H}}_{j,l_k}\bar{\mathbf{f}}_{j,l_k}\right)\right),\\
\mathbf{z}^{\mathsf{B}}_l &= \rho^{\mathsf{B}}_l g^{\mathsf{B}}_l\alpha_l\bar{\mathbf{h}}_{0,l}\mathbf{I}_L \otimes \left(\mathbf{e}^{\mathsf{T}}_l\mathbf{e}_l\right),\\
\mathbf{z}^{\mathsf{A}}_l &= \textstyle\sum_{k=1}^{K}\left(\rho^{\mathsf{A}}_{l_k}g^{\mathsf{A}}_{l_k}\bar{\mathbf{f}}_{l,l_k}\mathbf{I}_K \otimes \left(\mathbf{e}^{\mathsf{T}}_k\mathbf{e}_k\right)\right),\\
c^{\mathsf{B}}_l &= \ln\left(\rho^{\mathsf{B}}_l\right) - \rho^{\mathsf{B}}_l|g^{\mathsf{B}}_l|^2\left(\alpha_l\sigma^2 + \sigma^2_{l,r}\right) - \rho^{\mathsf{B}}_l + 1,\\
c^{\mathsf{A}}_l &= \textstyle\sum_{k=1}^{K}\left(\ln\left(\rho^{\mathsf{A}}_{l_k}\right) - \rho^{\mathsf{A}}_{l_k}|g^{\mathsf{A}}_{l_k}|^2\sigma^2 - \rho^{\mathsf{A}}_{l_k} + 1\right).
\end{aligned} \quad (21)$$

It is noted that since $\mathbf{X}^{\mathsf{B}}_l, \mathbf{X}^{\mathsf{A}}_{j,l}, \mathbf{X}^{\mathsf{SI}}_l, \mathbf{Y}^{\mathsf{B}}_l$ and $\mathbf{Y}^{\mathsf{A}}_{j,l}$ are semi-definite matrices, the optimization problem (17) with the constraints (20a)-(20c) is a convex QCQP. Therefore, the optimal $\mathbf{v}, \mathbf{w}_l$ and t_l with fixed $\theta_l, g^{\mathsf{B}}_l, \rho^{\mathsf{B}}_l, g^{\mathsf{A}}_{l_k}$ and $\rho^{\mathsf{A}}_{l_k}$ can be obtained by an existing interior-point method [13].

C. IRS Passive Beamforming Optimization

Let us define $Q = NL$, $\theta = [\theta^{\mathsf{H}}_1, \ldots, \theta^{\mathsf{H}}_L]^{\mathsf{H}} \in \mathbb{C}^{Q\times 1}$, $\mathbf{B}_{0,l} = [\mathbf{e}^{\mathsf{T}}_l \otimes \mathbf{A}^{\mathsf{H}}_{0,l,l}, \mathbf{h}^{d}_{0,l}{}^{\mathsf{H}}]^{\mathsf{H}}\mathbf{V}$, $\mathbf{B}_{\mathsf{SI},l} = [\mathbf{e}^{\mathsf{T}}_l \otimes \mathbf{A}^{\mathsf{H}}_{l,l,l}, \mathbf{h}^{d}_{l,l}{}^{\mathsf{H}}]^{\mathsf{H}}\mathbf{W}_l$, $\mathbf{B}_{j,l} = [\mathbf{e}^{\mathsf{T}}_j \otimes \mathbf{A}^{\mathsf{H}}_{j,j,l} + \mathbf{e}^{\mathsf{T}}_l \otimes \mathbf{A}^{\mathsf{H}}_{j,l,l}, \mathbf{h}^{d}_{j,l}{}^{\mathsf{H}}]^{\mathsf{H}}\mathbf{W}_j$, and $\mathbf{B}_{j,l_k} = [\mathbf{e}^{\mathsf{T}}_j \otimes \mathbf{A}^{\mathsf{ue}}_{j,l_k}{}^{\mathsf{H}}, \mathbf{f}^{d}_{j,l_k}{}^{\mathsf{H}}]^{\mathsf{H}}\mathbf{W}_j$. By using these notations, we can rewrite the constraints (17b), (17c) and (9e) with respect to θ, respectively, as

$$\theta^{\mathsf{H}}\mathbf{E}^{\mathsf{B}}_l\theta - 2\mathsf{Re}\{\theta^{\mathsf{H}}\mathbf{p}^{\mathsf{B}}_l\} + t_l\ln 2 \leq r^{\mathsf{B}}_l, \forall l \in \mathcal{L}, \quad (22)$$

$$\theta^{\mathsf{H}}\mathbf{E}^{\mathsf{A}}_l\theta - 2\mathsf{Re}\{\theta^{\mathsf{H}}\mathbf{p}^{\mathsf{A}}_l\} + t_l\ln 2 \leq r^{\mathsf{A}}_l, \forall l \in \mathcal{L}, \quad (23)$$

$$\theta^{\mathsf{H}}\mathbf{E}^{\mathsf{SI}}_l\theta + 2\mathsf{Re}\{\theta^{\mathsf{H}}\mathbf{p}^{\mathsf{SI}}_l\} + r^{\mathsf{SI}}_l \leq \eta_{\mathsf{ADC}}, \forall l \in \mathcal{L}. \quad (24)$$

where

$$\mathbf{C}^{\mathsf{B}}_l = \rho^{\mathsf{B}}_l|g^{\mathsf{B}}_l|^2\alpha_l\left(\mathbf{B}_{0,l}\mathbf{B}^{\mathsf{H}}_{0,l} + \textstyle\sum_{j\neq l}^{l}\mathbf{B}_{j,l}\mathbf{B}^{\mathsf{H}}_{j,l} + \beta_l\mathbf{B}_{\mathsf{SI},l}\mathbf{B}^{\mathsf{H}}_{\mathsf{SI},l}\right),$$

$$R^{\mathsf{B}}_l = \log_2\left(1+\gamma^{\mathsf{B}}_l\right) = \log_2\left(1 + \frac{\alpha^2_l|\bar{\mathbf{h}}_{0,l}\mathbf{v}_l|^2}{\alpha_l\beta_l|\bar{\mathbf{h}}_{0,l}\mathbf{v}_l|^2 + \sum_{j\neq l}^{L}\alpha_l|\bar{\mathbf{h}}_{0,l}\mathbf{v}_j|^2 + \sum_{j\neq l}^{L}\alpha_l\|\bar{\mathbf{h}}_{j,l}\mathbf{W}_j\|^2 + \alpha_l\beta_l\|\bar{\mathbf{h}}_{\mathsf{SI},l}\mathbf{W}_l\|^2 + \alpha_l\sigma^2 + \sigma^2_{\mathsf{r},l}}\right), \quad (7)$$

$$R^{\mathsf{A}}_{l_k} = \log_2\left(1+\gamma^{\mathsf{A}}_{l_k}\right) = \log_2\left(1 + \frac{|\bar{\mathbf{f}}_{l,l_k}\mathbf{w}_{l_k}|^2}{\sum_{m\neq k}^{K}|\bar{\mathbf{f}}_{l,l_k}\mathbf{w}_{l_m}|^2 + \sum_{j\neq l}^{L}\|\bar{\mathbf{f}}_{j,l_k}\mathbf{W}_j\|^2 + \|\bar{\mathbf{f}}_{0,l_k}\mathbf{V}\|^2 + \sigma^2}\right). \quad (8)$$

Authorized licensed use limited to: Univ Of Incheon. Downloaded on October 26,2026 at 13:13:39 UTC from IEEE Xplore. Restrictions apply.

Algorithm 1 BCD Algorithm for Obtaining MBS and SBS Precoder, and IRS Passive Beamforming

1: Initialize $T_{\max}$, ϵ, $\mathbf{V}$, $\mathbf{W}_l$, θ_i.
2: Set $n = 0$
3: **repeat**
4: Update $g_l^{\mathsf{B},n}$, $\rho_l^{\mathsf{B},n}$, $g_{l_k}^{\mathsf{A},n}$, and $\rho_{l_k}^{\mathsf{A},n}$.
5: Update $\mathbf{V}^n$ and $\mathbf{W}_l^n$ from solving QCQP
6: Update θ_l^n from solving problem (26)
7: Set $n = n + 1$
8: **until** the fractional increase of the objective value of (17a) is less than ϵ or $n = T_{\max}$

$$
\begin{aligned}
&\mathbf{C}_l^{\mathsf{A}} = \sum\nolimits_{k=1}^{K}\sum\nolimits_{j=1}^{L}\rho_{l_k}^{\mathsf{A}}|g_{l_k}^{\mathsf{A}}|^2\mathbf{B}_{j,l_k}\mathbf{B}_{j,l_k}^{\mathsf{H}}, \mathbf{C}_l^{\mathsf{SI}} = \mathbf{B}_{\mathsf{SI},l}\mathbf{B}_{\mathsf{SI},l}^{\mathsf{H}},\\
&\mathbf{E}_l^{\mathsf{B}} = \left[\mathbf{C}_l^{\mathsf{B}}\right]_{1:Q,1:Q}, \mathbf{E}_l^{\mathsf{A}} = \left[\mathbf{C}_l^{\mathsf{A}}\right]_{1:Q,1:Q}, \mathbf{E}_l^{\mathsf{SI}} = \left[\mathbf{C}_l^{\mathsf{SI}}\right]_{1:Q,1:Q},\\
&\mathbf{d}_l^{\mathsf{B}} = \rho_l^{\mathsf{B}} g_l^{\mathsf{B}}\alpha_l\mathbf{B}_{0,l}\mathbf{e}_l, \mathbf{d}_l^{\mathsf{A}} = \sum\nolimits_{k=1}^{K}\rho_{l_k}^{\mathsf{A}} g_{l_k}^{\mathsf{A}}\mathbf{B}_{l,l_k}\mathbf{e}_k,\\
&\mathbf{p}_l^{\mathsf{B}} = \left[\mathbf{d}_l^{\mathsf{B}}\right]_{1:Q} - \left[\mathbf{C}_l^{\mathsf{B}}\right]_{1:Q,Q+1}, \mathbf{p}_l^{\mathsf{A}} = \left[\mathbf{d}_l^{\mathsf{A}}\right]_{1:Q} - \left[\mathbf{C}_l^{\mathsf{A}}\right]_{1:Q,Q+1},\\
&\mathbf{p}_l^{\mathsf{SI}} = \left[\mathbf{C}_l^{\mathsf{SI}}\right]_{1:Q,Q+1}, r_l^{\mathsf{SI}} = \left[\mathbf{C}_l^{\mathsf{SI}}\right]_{Q+1,Q+1},\\
&r_l^{\mathsf{B}} = \ln\left(\rho_l^{\mathsf{B}}\right) - \rho_l^{\mathsf{B}}|g_l^{\mathsf{B}}|^2\left(\alpha_l\sigma^2 + \sigma_{l,r}^2\right) - \rho_l^{\mathsf{B}} + 1 - \left[\mathbf{C}_l^{\mathsf{B}}\right]_{Q+1,Q+1}\\
&\qquad +2\mathsf{Re}\left(\left[\mathbf{d}_l^{\mathsf{B}}\right]_{Q+1}\right),\\
&r_l^{\mathsf{A}} = \sum\nolimits_{k=1}^{K}\left(\ln\left(\rho_{l_k}^{\mathsf{A}}\right) - \rho_{l_k}^{\mathsf{A}}|g_{l_k}^{\mathsf{A}}|^2\left(\|\bar{\mathbf{f}}_{0,l_k}\mathbf{V}\|^2+\sigma^2\right) - \rho_{l_k}^{\mathsf{A}} + 1\right)\\
&\qquad -\left[\mathbf{C}_l^{\mathsf{B}}\right]_{Q+1,Q+1} + 2\mathsf{Re}\left(\left[\mathbf{d}_l^{\mathsf{A}}\right]_{Q+1}\right),
\end{aligned}
\tag{25}
$$

Note that (22), (23), and (24) are convex, but (9e) is still non-convex constraint. To address this difficulty, by defining $\hat{\theta} = [\theta^{\mathsf{H}}, 1]^{\mathsf{H}}$ and $\Phi = \hat{\theta}\hat{\theta}^{\mathsf{H}}$, we first reformulate (17) with the constraints (22)-(24) with respect to Φ as

$$
\begin{aligned}
\max_{t_l,\breve{}} \quad & \sum_{l=1}^{L} t_l && \text{(26a)}\\
\text{s.t.} \quad & \mathsf{Tr}\left(\mathbf{Q}_l^{\mathsf{B}}\breve{}\right) + t_l\ln 2 \le r_l^{\mathsf{B}},\ \forall l\in\mathcal{L}, && \text{(26b)}\\
& \mathsf{Tr}\left(\mathbf{Q}_l^{\mathsf{A}}\breve{}\right) + t_l\ln 2 \le r_l^{\mathsf{A}},\ \forall l\in\mathcal{L}, && \text{(26c)}\\
& \mathsf{Tr}\left(\mathbf{Q}_l^{\mathsf{SI}}\breve{}\right) + t_l\ln 2 \le \eta_{\mathsf{ADC}},\ \forall l\in\mathcal{L}, && \text{(26d)}\\
& \breve{} \succeq 0, \mathsf{Rank}(\breve{}) = 1, && \text{(26e)}\\
& [\breve{}]_{q,q} = 1, q = 1,\ldots,Q+1. && \text{(26f)}
\end{aligned}
$$

where

$$
\mathbf{Q}_l^{\mathsf{B}} = \begin{bmatrix}\mathbf{C}_l^{\mathsf{B}} & \mathbf{d}_l^{\mathsf{B}}\\ \mathbf{d}_l^{\mathsf{B}\mathsf{H}} & 0\end{bmatrix}, \mathbf{Q}_l^{\mathsf{A}} = \begin{bmatrix}\mathbf{C}_l^{\mathsf{A}} & \mathbf{d}_l^{\mathsf{A}}\\ \mathbf{d}_l^{\mathsf{A}\mathsf{H}} & 0\end{bmatrix}, \mathbf{Q}_l^{\mathsf{SI}} = \begin{bmatrix}\mathbf{C}_l^{\mathsf{SI}} & \mathbf{d}_l^{\mathsf{SI}}\\ \mathbf{d}_l^{\mathsf{SI}\mathsf{H}} & 0\end{bmatrix}. \tag{27}
$$

By relaxing the rank-one constraint (26e), (26) can be transformed into a conventional semidefinite programming (SDP), which can be solved using CVX. To obtain a sub-optimal solution $\theta^\star$ from $\breve{}^\star$, we adopt Gaussian randomization method [14]. In the $(n+1)$-th iteration, we update $\theta^{n+1} = \theta^n$ if the objective value with $\theta^\star$ is smaller than the value with θ^n, otherwise $\theta^{n+1} = \theta^\star$, which ensures a non-decreasing objective value over iterations.

The detailed description of our proposed algorithm is presented in Algorithm 1. At each iteration, $g_l^{\mathsf{B},n}$, $\rho_l^{\mathsf{B},n}$, $g_{l_k}^{\mathsf{A},n}$, and $\rho_{l_k}^{\mathsf{A},n}$ are updated as (18) and (19), and $\mathbf{V}$ and $\mathbf{W}$ are then updated by solving QCQP, while θ_l is updated by solving the problem (26). The algorithm continues until the objective function (17a) converges. Note that the objective function in (17) is non-decreasing over iterations and converges to a local optimal value, since the system sum rate in (9a) has an upper bound due to the limited transmit power of MBS and SBSs, and the finite number of IRS elements.

The main complexity of the proposed algorithm arises from steps 5 and 6 in Algorithm 1. The complexity of solving QCQP problem is $\mathcal{O}(9m^{0.5}L^{2.5}(m+3L)\ln(\frac{2mV}{\varepsilon}))$, where $m = N_{\mathsf{M}} + N_{\mathsf{S}}K$, V is a constant defined in [13] with $V > \varepsilon$, while the complexity of solving SDP problem is $\mathcal{O}((3L+N_{\mathsf{I}}L+2)^{3.5})$ [14]. Therefore, the overall complexity of Algorithm 1 is $\mathcal{O}(I_1(9m^{0.5}L^{2.5}(m+3L)\ln(\frac{2mV}{\varepsilon})+(3L+N_{\mathsf{I}}L+2)^{3.5}))$.

IV. Simulation Results

In this section, we evaluate our proposed algorithm via numerical results. In the network under consideration, MBS is located at the center [0 m, 0 m], 3 SBSs are deployed at [200 m, 0 m], [−100 m, $100\sqrt{3}$ m] and [−100 m, $-100\sqrt{3}$ m], and 4 UEs are randomly deployed within each SBS cell with a radius of 40m. Each IRS is deployed at a distance of d_{I} from each SBS and it has a square shape satisfying $N_{\mathsf{I}} = N^2$, where N is the number of elements in each axis. Unless specifically stated, for system parameters, we set $N_{\mathsf{M}} = 12, N_{\mathsf{S}} = 4, P_{\mathsf{M}} = 46\,\text{dBm}, P_{\mathsf{S}} = 30\,\text{dBm}, \sigma^2 = -90\,\text{dBm}, \sigma_{\mathsf{r}}^2 = -110\,\text{dB}, d_{\mathsf{I}} = 0.5\,\text{m}, b = 11$, and $f_c = 2.4\,\text{GHz}$ as an example. We adopt Rician channel model with a Rician factor of 3dB for BS-UE and SBS-UE channels. In the SI channel, LoS path is modeled using a near-field model, while NLoS paths are modeled by a far-field model with a Rician factor of 30dB. For comparison, we use the following benchmark schemes:

- *SImin+ZF* [6]: The passive beamforming of each IRS is designed to minimize SI power, and zero-forcing (ZF) precoder is used at MBS and each SBS.
- *SImin+WMMSE:* The proposed WMMSE method is used for MBS and SBS precoders, while IRS passive beamforming is optimized for minimizing SI power.
- *RelaxProj*: Relaxation and projection method in [15] is used for obtaining IRS passive beamforming
- *FD* ($b = \infty$)*:* All SBSs operate in FD mode with infinite ADC bits.
- *HD:* All SBSs operate in half-duplex (HD) mode with infinite ADC bits.
- *noIRS:* All SBSs operate in FD mode without IRS.

Fig. 2(a) presents the convergence of the Algorithm 1. As shown in Fig. 1(a), the sum rate performance of Algorithm 1 monotonically increases over iterations and converge to a local optimal value within 50 iterations for different value of N_{I}, showing the robustness of the proposed algorithm.

Fig. 2(b) shows the sum rate performance versus the number of IRS elements N_{I}. It is worth noting that deploying IRS can definitely mitigate self-interference compared to w/o IRS, facilitating the implementation of FD communication. Moreover, the proposed algorithm suppresses the overall interference including cross-tier interference, inter-SBS/cell interference, and self-interference compared with SImin+ZF scheme which minimizes only self-interference with the help of IRS and intra-cell interference with ZF precoder. It can be also observed that SImin+WMMSE scheme enhances the sum rate performance due to employing the proposed

Authorized licensed use limited to: Univ Of Incheon. Downloaded on October 26,2026 at 13:13:39 UTC from IEEE Xplore. Restrictions apply.

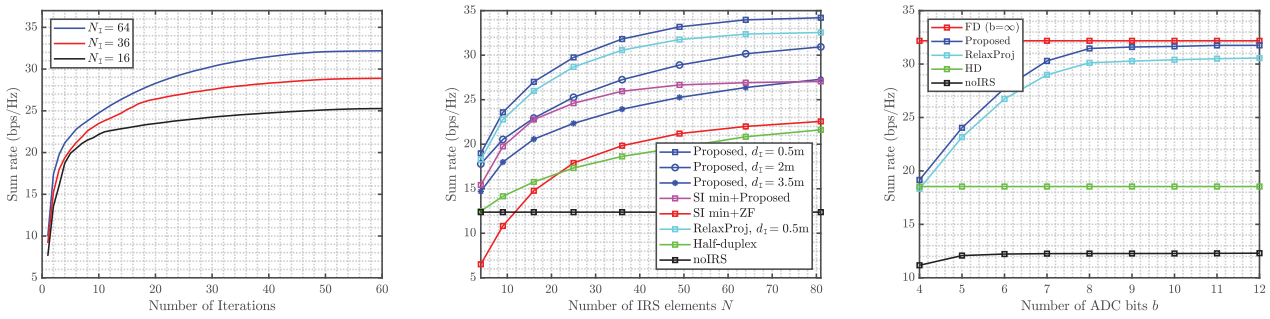


Fig. 2. (a) Convergence behavior of Algorithm 1 with different number of IRS elements N_I, (b) Sum rate vs. Number of IRS elements with $b = 11$, (c) Sum rate vs. Number of ADC bits with $N_\mathrm{I} = 36$.

WMMSE algorithm, but it cannot efficiently exploit the benefits of IRSs by only minimizing self-interference, resulting in performance degradation. This results verify the effectiveness of our proposed algorithm, which has the ability to strike a balance between enhancing channel gain and mitigating network interference by exploiting the characteristics of IRSs.

Furthermore, it can be confirmed that three design parameters affect the system performance. Firstly, as shown in Fig. 2(b), the sum rate increases with the number of IRS elements N_I. This is because installing IRS with large N_I can utilize more degree-of-freedom (DoF) to enhance channel gain and mitigate network interference while satisfying ADC constraint (9d). Secondly, the sum rate decreases with the increase in the distance between SBS and IRS d_I. It can be inferred that deploying IRS in close proximity to SBS is essential to achieve maximum performance gain. Lastly, as illustrated in Fig. 2(c), ADC quantization bits b highly affect the system sum rate performance. Compared to w/o IRS scheme where the precoder at the SBS is fully exploited to meet ADC dynamic range constraint, the proposed algorithm can easily satisfy ADC constraint with the help of IRS and allow for better interference mitigation, resulting in improvement of sum rate. With the increase of b, the sum rate of the proposed scheme is increased and saturated. Since the ADC dynamic range is enough to be feasible with high value of b, the remaining DoF would be used for enhancing channel gain and mitigating other interference powers. It can be concluded that with the assistance of IRSs, 8-bit ADC is enough to achieve the performance of ideal FD system without using a large number of ADC bits. Note that a large number of ADC bits requires high power consumption and high implementation cost. Thus, the proposed algorithm can resolve these drawbacks by using lower ADC bits with the help of IRS. We believe that these insights can provide network design guidance when deploying IRS near SBS and implementing ADC at SBS for FD system.

V. Conclusion

In this letter, we studied the joint active/passive beamforming in the IRS-aided FD IAB network, where IRS is deployed in the vicinity of each SBS to mitigate self-interference and network interference. We proposed the WMMSE-based BCD optimization framework to maximize the system sum rate, where the precoders of MBS and SBSs are obtained by transforming it into QCQP problem, and IRS passive beamforming is optimized by using SDR. Simulation results demonstrated that deploying IRS can effectively mitigate interference and showed that our proposed algorithm with 8-bit ADC achieves nearly double sum rate compared to HD IAB network.

References

[1] G. Y. Suk et al., "Full duplex integrated access and Backhaul for 5G NR: Analyses and prototype measurements," *IEEE Wireless Commun.*, vol. 29, no. 4, pp. 40–46, Aug. 2022.

[2] E. Chen, M. Tao, and N. Zhang, "User-centric joint access-Backhaul design for full-duplex self-Backhauled wireless networks," *IEEE Trans. Commun.*, vol. 67, no. 11, pp. 7980–7993, Nov. 2019.

[3] J. Zhou, T. -H. Chuang, T. Dinc, and H. Krishnaswamy, "Integrated wideband self-interference cancellation in the RF domain for FDD and full-duplex wireless," *IEEE J. Solid-State Circuits*, vol. 50, no. 12, pp. 3015–3031, Dec. 2015.

[4] Q. Wu, S. Zhang, B. Zheng, C. You, and R. Zhang, "Intelligent reflecting surface-aided wireless communications: A tutorial," *IEEE Trans. Commun.*, vol. 69, no. 5, pp. 3313–3351, May 2021.

[5] X. Pang, W. Mei, N. Zhao, and R. Zhang, "Intelligent reflecting surface assisted interference mitigation for cellular-connected UAV," *IEEE Wireless Commun. Lett.*, vol. 11, no. 8, pp. 1708–1712, Aug. 2022.

[6] W. Zhang, Z. Wen, C. Du, Y. Jiang, and B. Zhou, "RIS-assisted self-interference mitigation for in-band full-duplex transceivers," *IEEE Trans. Commun.*, vol. 71, no. 9, pp. 5444–5454, Sep. 2023.

[7] C. Qiu et al., "Intelligent reflecting surface empowered self-interference cancellation in full-duplex systems," *IEEE Trans. Commun.*, early access, Dec. 27, 2023, doi: 10.1109/TCOMM.2023.3347576.

[8] L. Wei et al., "Channel estimation for RIS-empowered multi-user MISO wireless communications," *IEEE Trans. Commun.*, vol. 69, no. 6, pp. 4144–4157, Jun. 2021.

[9] A. J. Fernandes and I. Psaromiligkos, "Channel estimation for reconfigurable intelligent surface-assisted full-duplex MIMO with hardware impairments," *IEEE Wireless Commun. Lett.*, vol. 12, no. 10, pp. 1697–1701, Oct. 2023.

[10] G. Y. Suk et al., "Dynamic RF beam codebook reduction for cost-efficient mmWave full-duplex systems," in *Proc. IEEE Glob. Commun. Conf. (GLOBECOM)*, 2022, pp. 1–6.

[11] Y. Lu, K. Xiong, P. Fan, B. Ai, and Z. Zhong, "Outage-constrained sum transmission rate maximization in RIS-assisted MISO systems," *IEEE Trans. Wireless Commun.*, vol. 23, no. 4, pp. 2505–2518, Apr. 2024.

[12] S. S. Christensen, R. Agarwal, E. De Carvalho, and J. M. Cioffi, "Weighted sum-rate maximization using weighted MMSE for MIMO-BC beamforming design," *IEEE Trans. Wireless Commun.*, vol. 7, no. 12, pp. 4792–4799, Dec. 2008.

[13] Y. Nesterov and A. Nemirovskii, *Interior-Point Polynomial Algorithms in Convex Programming*. Philadelphia, PA, USA: SIAM, 1994.

[14] M. Hua, Q. Wu, D. W. K. Ng, J. Zhao, and L. Yang, "Intelligent reflecting surface-aided joint processing coordinated multipoint transmission," *IEEE Trans. Commun.*, vol. 69, no. 3, pp. 1650–1665, Mar. 2021.

[15] S. Fang, G. Chen, P. Xiao, K.-K. Wong, and R. Tafazolli, "Intelligent Omni surface-assisted self-interference cancellation for full-duplex MISO system," *IEEE Trans. Wireless Commun.*, vol. 23, no. 3, pp. 2268–2281, Mar. 2024.

Authorized licensed use limited to: Univ Of Incheon. Downloaded on October 26,2026 at 13:13:39 UTC from IEEE Xplore. Restrictions apply.